A STUDY OF THE NORTHWESTERN PACIFIC UPPER MANTLE

A THESIS SUBMITTED TO THE GRADUATE SCHOOL OF THE
UNIVERSITY OF HAWAII IN PARTIAL FULFILLMENT
OF THE REQUIREMENTS FOR THE DEGREE OF
MASTER OF SCIENCE IN GEOLOGICAL SCIENCE
(GEOPHYSICS)
JUNE 1965

By

Daniel Alvin Walker

Thesis Committee:

Wm. Mansfield Adams, Chairman
Augustine S. Furumoto
John C. Rose
Ralph M. Moberly Jr.
Klaus Wyrtki

We certify that we have read this thesis and that in our opinion it is satisfactory in scope and quality as a thesis for the degree of Master of Science in Geological Science (Geophysics).

THESIS COMMITTEE

Wm. Mansfield Adams
Chairman

Augustus S. Furumoto

John C. Rose

Noah Mokelke

Thomas Yamaki

Contents

Abstract

A fundamental problem of earthquake seismology is the occurrence of the upper mantle low-velocity channel. This study is intended to confirm or deny its existence in the upper mantle below the Northwestern Pacific on the basis of body wave arrivals at a bottom-mounted hydrophone near Wake Island. A comparison of the observed travel times shows an extreme anomaly in the apparent surface distance range of twenty-one to thirty-three degrees for both P and S waves. Assumed linear paths suggest a P wave channel upper boundary between 165 km and 185 km, and a lower boundary between 290 km and 542 km. Travel times for P and S waves indicate that the velocities in the channel remain constant at 8.1 km/sec and 4.65 km/sec respectively.

Introduction

Records obtained with a bottom-mounted hydrophone at Wake Island are used in this study for an analysis of P and S waves originating from the Marianas Islands, Japan, and the Southern Kurils Islands. Because the distances for these areas range from 18 degrees for the Marianas to 30 degrees for the Kurils, P and S arrivals at Wake are ideal for studying the effect of the "20-degree discontinuity". A Map showing the relation of the epicenter areas to the bottom-mounted hydrophone location is shown in Figure 1.

The objective of the study was to obtain evidence for the low-velocity channel below the Northwestern Pacific on the basis of P and S arrivals at Wake from the above-mentioned areas. If adequate evidence were found, it was hoped that the data might permit the boundaries of the channel to be established from an analysis of the

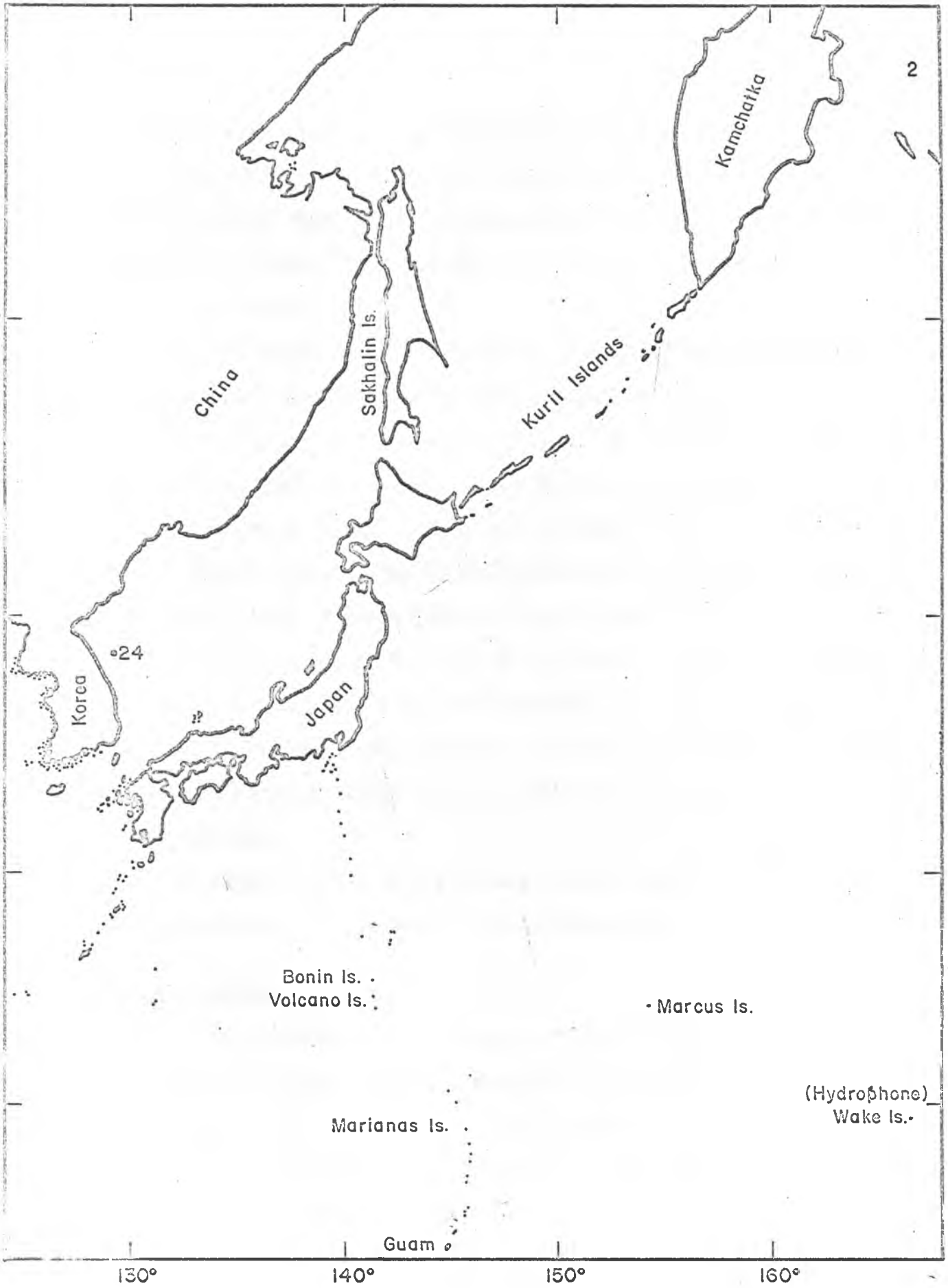

Fig. 1. Northwestern Pacific

observed velocities as a function of distance and depth.

Prior to this study, the only seismic data related to the Northwestern Pacific Upper Mantle structure was obtained from surface wave dispersion studies. The following is a summary of these studies and their conclusions.

Dorman, Ewing, and Oliver (1960) said that multilayer dispersion computations indicated a very prominent region of low shear velocity between depths of about 100 and 200 km under the continents, and from 60 to 100 km under the oceans. At the Pacific Science Congress held at the University of Hawaii, Ewing, Brune, and Kuo (1962) proposed a low shear velocity channel from 60 to 150 km under the Pacific. Anderson and Toksoz (1963) proposed spherical models which satisfy Love wave and torsional oscillation data. A low shear velocity channel in the 75 to 160 km depth range with a velocity of about 4.35 km/sec is suggested. Kovach and Anderson (1964) found that under the Pacific the low velocity shear wave zone may extend to 400 km followed by an abrupt increase in shear velocity.

It should be noted that the above studies were made for the Pacific in general and not specifically for the Northwestern Pacific.

P and S Arrivals

A first step was the establishment of the validity of the phases as P and S arrivals. This was necessary as there was a possibility that the pressure level recordings could be T phases which arrived at the same time as the expected P and S arrivals. The criteria which were employed for eliminating T phases were:

1. All T phases recorded on the bottom-mounted hydrophone would

be expected to also be recorded on the hydrophone mounted at the axis of the sound channel. Phases not recorded on the channel-mounted hydrophone, therefore, would presumably not be T phases.

2. The low probability of random T phases being recorded at the same general time as the expected P and S arrivals for 27 events further substantiated that the observed phases were not T phases.

Because the arrival times of the phases often were later than the expected P and S arrivals, there was also the possibility that the phases were PP and SS arrivals rather than P and S arrivals. However, confusion on this point could be resolved on the basis of the following:

1. The travel times indicated that if the phases were PP and SS arrivals, they arrived from 20 to 50 seconds early.
2. If PP and SS arrivals were recorded, at least some corresponding P and S arrivals should have been observed in the range from 18 to 63 degrees, because of their higher energy. As such phases were not observed prior to the first arrivals for any of the 27 events studied, it was reasonable to conclude that the arrivals were neither PP's nor SS's.
3. The observed phase intervals fitted very poorly to the Jeffreys-Bullen (1958) SS-PP arrival intervals, whereas there was a good fit to the Jeffreys-Bullen S-P intervals as shown in Table 1.

All lines of evidence therefore indicated that the phases were neither T nor PP or SS arrivals and as the phase intervals and observed travel times corresponded closely to those to be expected for P and S arrivals, one could safely conclude that the arrivals were actually P

Table 1. Travel Time Intervals

Event No.	J-B SS-PP (secs.)	J-B S-P (secs.)	Observed Interval (secs.)
1	209	199.0	199.0
2	218	206.5	190.0
3	226	210.0	189.0
4	236	226.5	213.0
5	236	226.5	213.0
6	-	-	-
7	249	229.5	230.5
8	-	-	-
9	256	239.5	233.0
10	272	248.5	246.0
11	276	253.0	244.0
12	-	-	-
13	310	277.5	272.0
14	312	277.5	278.0
15	315	280.5	277.0
16	-	-	-
17	318	282.0	280.0
18	319	282.0	285.0
19	321	284.5	287.0
20	-	-	-
21	325	280.0	291.0
22	333	292.0	303.0
23	364	311.5	327.0

and S phases.

Presentation of the Data

Of the approximately fifty events that were recorded from August 1963 to August 1964, twenty-seven were chosen for this study, the only criterion used for selection being the clarity of the first arrivals. The P and S arrivals of these twenty-seven events are shown in Figure 2. The times at which the P and S arrivals were read are indicated by arrows. In most cases the first-arriving S waves were partly obscured by the later-arriving P's, and hence the reliability of S arrivals is debatable.

Through the courtesy of the Coast and Geodetic Survey, the origin times, coordinates, and focal depths of all the earthquakes used were recomputed to give maximum precision. These data are given in Table 2. Coordinates and depths are accurate to within ± 0.1 degree and ± 10 km respectively. Figure 3 is a map of the epicenter positions.

A comparison between the observed travel times and the Jeffreys-Bullen travel times clearly indicates an anomaly in the 21 to 33-degree range. Apparent distances as measured on the surface of the earth, depths, interpolated Jeffreys-Bullen travel times, observed travel times, and residuals are listed in Table 3.

Although the P and S residuals are significant in the 21 to 33-degree range, this is not necessarily indicative of a low-velocity channel. It merely shows that the velocities are less than those predicted by the Jeffreys-Bullen tables. As depth increases from 33 km to 450 km, the Jeffreys-Bullen velocity values increase linearly from 7.7 km/sec to 9.0 km/sec for compressional waves and from 4.3 km/sec to 5.0 km/sec for shear waves. Therefore, the P and S residuals only indicate

1.
Origin Time
17:58:15.7

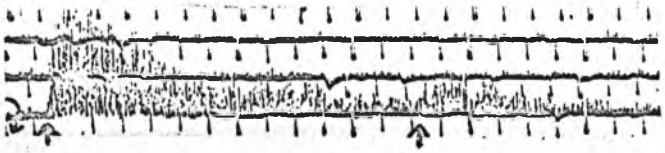

P at 18:02:23 S at 18:05:33

2.

20:40:34.8

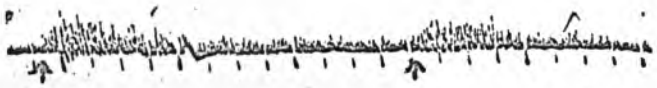

P at 20:44:52 S at 20:48:02

3.

06:06:45

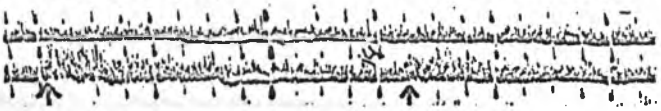

P at 06:11:06 S at 06:14:15

4.

01:15:27.2

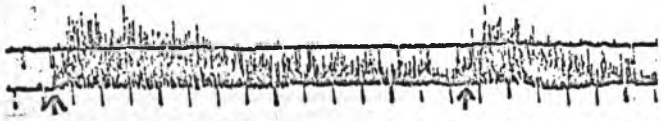

P at 01:20:06 S at 01:23:38

5.

04:12:38.9

P at 04:17:13 S at 04:20:36

6.

17:20:13.4

P at 17:25:08 S is not clear.

7.

13:10:05.4

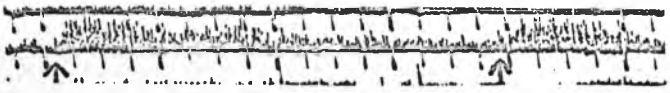

P at 13:15:06 S at 13:18:55

8.

03:58:48.9

P at 04:03:52 S is not clear.

9.

13:17:47.1

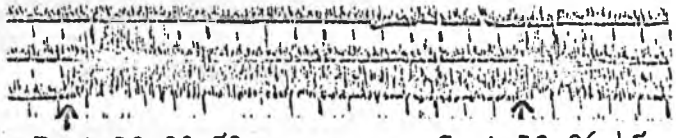

P at 13:22:52 S at 13:26:45

10.

22:00:58.9

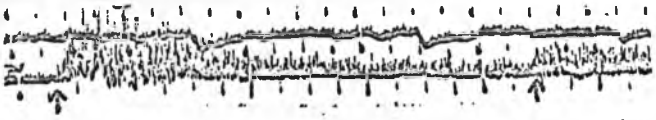

P at 22:06:22 S at 22:10:28

11.

05:39:42.6

P at 05:45:12 S at 05:49:16

12.

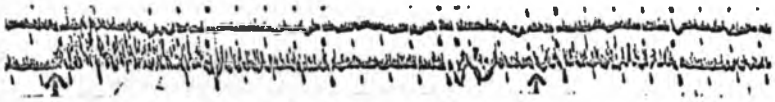

15:51:06.3 P at 15:56:38 S is not clear.

13.

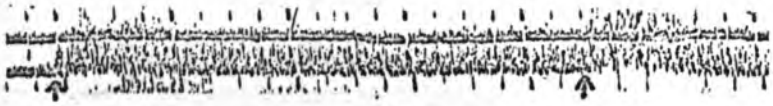

13:21:42.2 P at 13:27:56 S at 13:32:28

14.

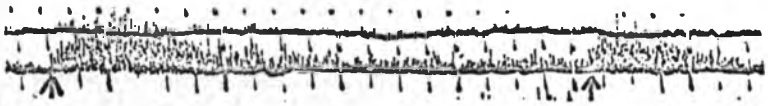

11:30:15.7 P at 11:36:30 S at 11:41:08

15.

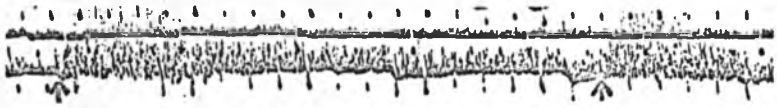

21:06:32.4 P at 21:12:53 S at 21:17:30

16.

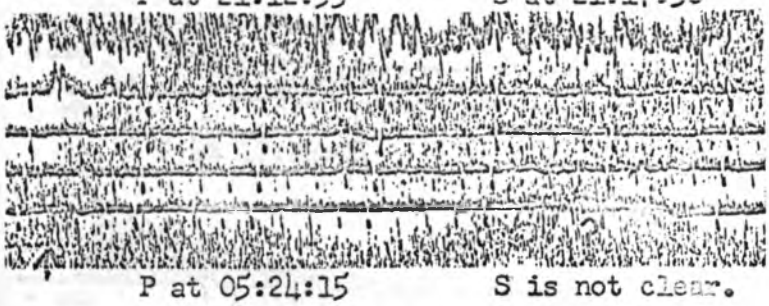

05:17:57.1 P at 05:24:15 S is not clear.

17.

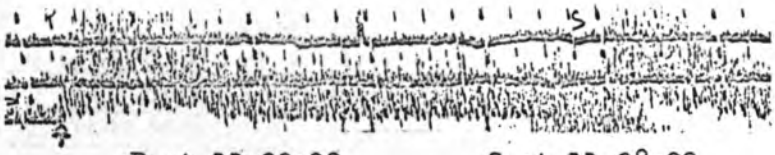

11:26:58.1 P at 11:33:20 S at 11:38:00

18.

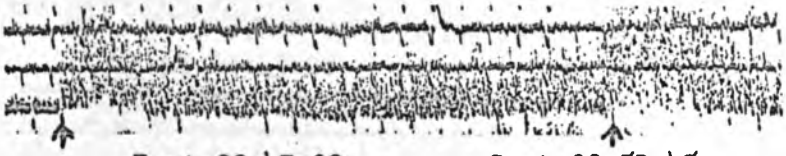

00:40:36.4 P at 00:47:00 S at 00:51:45

19.

16:11:00.2 P at 16:17:22 S at 16:22:09

20.

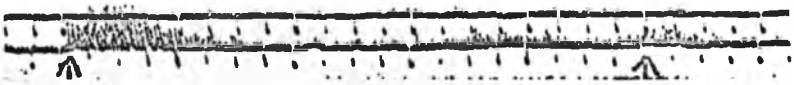

01:54:33.5 P at 02:01:05 S is not clear.

21.

23:24:41.8 P at 23:31:04 S at 23:35:55

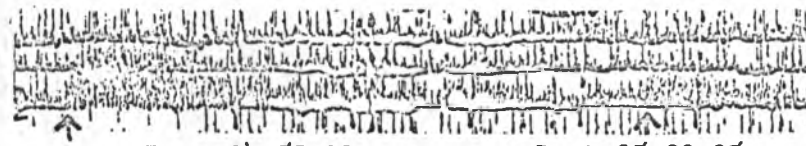

22.

04:50:53.8 P at 04:57:32 S at 05:02:35

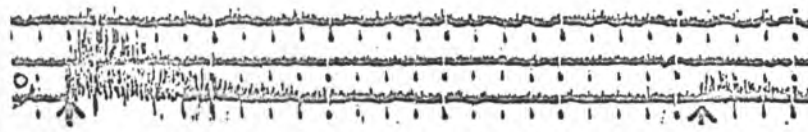

23.

12:03:22.5 P at 12:10:46 S at 12:16:13

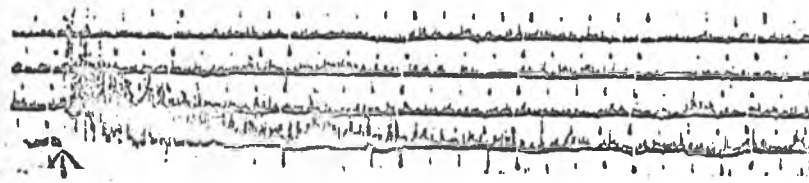

24.

17:17:45.5 P at 17:24:08 S is not present.

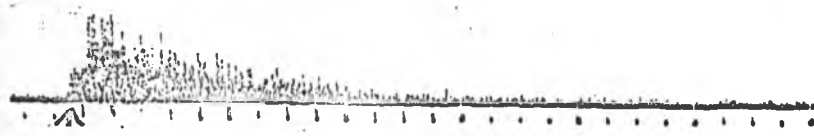

25.

00:30:02.6 P at 00:38:38 S is not present.

26.

03:36:12.7 P at 03:45:28 S is not present.

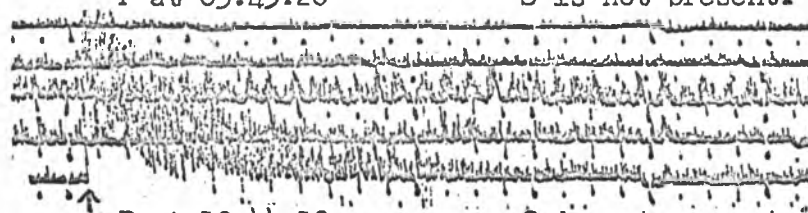

27.

19:34:45.5 P at 19:44:10 S is not present.

Fig. 2. P and S Arrivals

Table 2. United States Coast and Geodetic Survey Data

Event #	Date	Time	Coordinates	Depth	Mag.
1	Jan. 22, 1964	17:58:15.7	20.2N, 147.1E	32	5.1
2	Aug. 27, 1963	20:40:34.8	18.4N, 146.6E	56	4.1
3	Dec. 11, 1963	06:06:45	19.6N, 145.7E	110	4.5
4	Dec. 30, 1963	01:15:27.2	21.5N, 144.4E	145	5.2
5	Dec. 17, 1963	04:12:38.9	22.2N, 144.3E	105	4.4
6	Jan. 30, 1964	17:20:13.5	23.3N, 143.4E	33	4.7
7	April 10, 1964	13:10:04.1	13.5N, 144.5E	98	5.4
8	Nov. 14, 1963	03:58:48.9	22.6N, 142.9E	178	4.9
9	Aug. 10, 1963	13:17:46.1	24.4N, 142.7E	33	5.0
10	Sept. 7, 1963	22:00:57.1	27.5N, 141.5E	46	4.9
11	May 10, 1964	05:39:39.9	29.1N, 141.6E	36	5.3
12	Aug. 28, 1963	15:51:04.3	28.2N, 141.0E	83	5.1
13	Oct. 14, 1963	13:21:42.2	44.9N, 151.1E	33	5.9
14	Feb. 5, 1964	11:30:16.2	36.5N, 140.9E	52	5.4
15	Nov. 15, 1963	21:06:32.4	44.4N, 149.0E	33	6.0
16	Oct. 13, 1963	05:17:57.1	44.8N, 149.5E	52	8
17	Oct. 12, 1963	11:26:58.1	44.7N, 149.1E	39	6.5
18	May 31, 1964	00:40:39.2	43.6N, 146.9E	68	6.3
19	May 2, 1964	16:11:01.0	45.5N, 150.5E	37	5.7
20	May 3, 1964	01:54:33.8	40.3N, 141.8E	62	4.8
21	Dec. 12, 1963	23:24:41.8	46.3N, 150.6E	134	5.2
22	Jan. 10, 1964	04:50:53.8	41.9N, 142.6E	38	5.5
23	Oct. 28, 1963	12:03:22.5	52.8N, 160.0E	57	4.4
24	Jan. 24, 1964	17:17:45.5	38.7N, 129.4E	542	5.3
25	Dec. 18, 1963	00:30:02.6	24.8S, 176.6W	46	6.5
26	March 28, 1964	03:36:12.7	61.1N, 147.6W	20	8.5
27	Dec. 15, 1963	19:34:45.8	4.8S, 108.0E	660	6.4

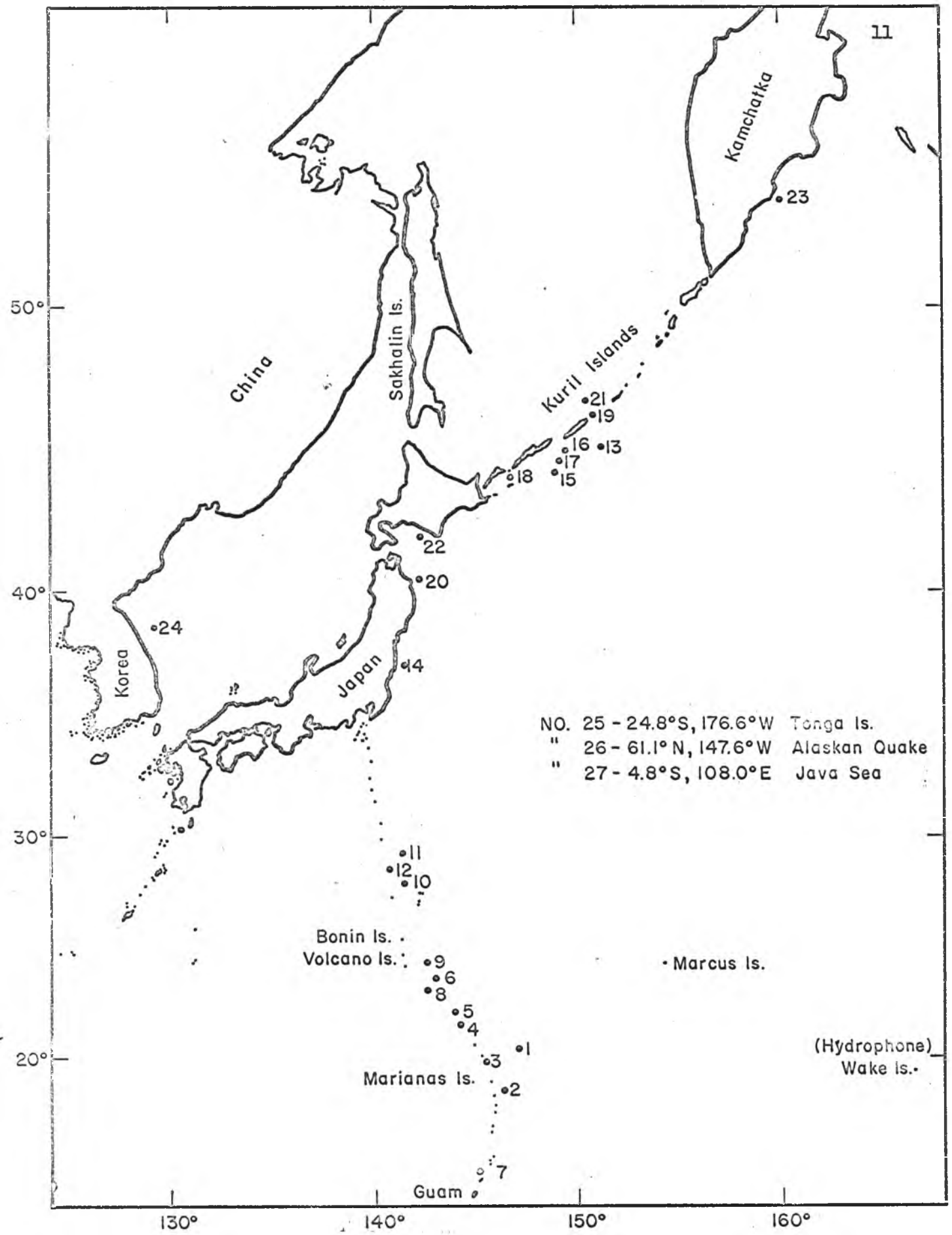

Fig. 3. Epicenter Map

Table 3. Observed Arrivals and Residuals

Event No.	Apparent Distance (degrees)	Depth (km)	P Travel Time J - B (secs.)	P Travel Time Observed (secs.)	P Travel Time Residuals (secs.)	S Travel Time J - B (secs.)	S Travel Time Observed (secs.)	S Travel Time Residuals (secs.)
1	18.2	32	251.5	247.5	-4	450.5	437.5	-13
2	19.0	56	260	257	-3	466.5	447	-19.5
3	19.6	110	262	261	-1	472	450	-22
4	20.6	145	269.5	279	+9.5	500	491	-9
5	20.7	105	274	274	0	500.5	487	-13.5
6	21.8	33	291	291	0	--	NC	--
7	21.8	98	285.5	297.5	+12	515	528	+13
8	22.3	178	283	303	+20	--	NC	--
9	22.5	33	298	304	+6	537.5	537	-0.5
10	24.1	46	312	323	+11	560.5	569	+8.5
11	24.4	36	314	327	+13	567	571	+4
12	24.5	83	311.5	329.5	+18	--	NC	--
13	27.6	33	346.5	374	+27.5	624	646	+22
14	27.7	52	346	375	+29	623.5	653	+29.5
15	28.0	33	350	380.5	+30.5	630.5	657.5	+27
16	28.1	60	348	378	+30	--	NC	--
17	28.3	39	352	382	+30	634	662	+28
18	28.4	68	352.5	386.5	+34	634.5	671.5	+37
19	28.6	37	355.5	383	+27.5	640	670	+30
20	28.8	62	354.5	392	+37.5	--	NC	--
21	29.0	134	349	382	+33	629	673	+44
22	29.7	38	364.5	398	+33.5	656.5	701	+44.5
23	32.7	57	389.5	443.5	+54	701	770.5	+69.5
24	37.0	542	385	382.5	-2.5	--	NP	--
25	48.0	46	516.5	515.5	-1	--	NP	--
26	51.7	20	551	555.5	+4.5	--	NP	--
27	63.0	660	567.5	565	-2.5	--	NP	--

NC - not clear
NP - not present

a velocity gradient less than the predicted values using the Jeffreys-Bullen tables.

A Modified Time-Distance Relation

In studies of the low-velocity channel, travel times are customarily plotted against apparent distances - the distance as measured on the surface of the earth from the epicenter to the recording station. This method of plotting is only acceptable, however, if all events are of nearly the same focal depth. Because the foci in this study varied considerably in depth, an adjustment has to be made. In order to achieve this, distances as measured along a linear path through the earth from the focus to the recording station were used rather than apparent distances. These chord segment distances are preferable to the apparent distances since they decrease with increasing focal depth, as is the case with the actual travel path, while apparent distances are independent of the focal depth. It should be emphasized that chord segment distances do not entirely eliminate the effect of focal depth but are merely preferable to apparent distances.

Foci were plotted to scale on a large arc corresponding to earth curvature at the approriate apparent distances and depths (Figure 4).

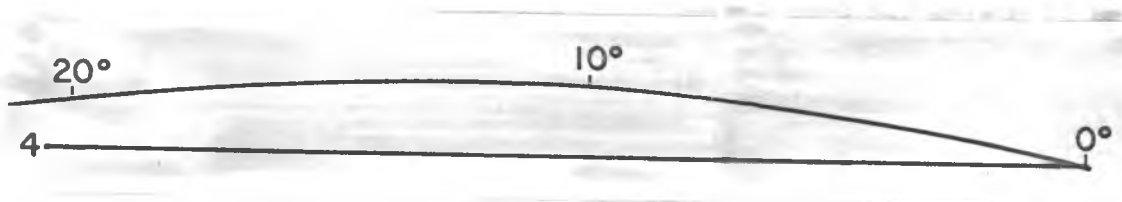

Fig. 4. Chord Segment Distances

The linear distances were then measured from the foci to the station to obtain the chord-segment distances. Table 4 contains the chord-segment distances, the P and S travel times, and the expected Jeffreys-Bullen travel times for events 1 through 27. Figures 5 and 6 are plots of the observed and expected P and S travel times versus chord segment distances.

The Velocity Variation in the Mantle

For distances less than 20-degrees, the observed and expected P travel times show a close correspondence. As the events become more distant, discrepancies appear and increase. Beyond a chord-segment distance of 32.1 degrees, the expected and observed travel times again show a close correspondence. The sharp drop in the observed travel times of events occurring at 32.1 degrees and 35.1 degrees indicates that a very rapid increase in velocity must have occurred.

Considering a possible 5-second error in reading first arrivals, nearly all the data points could be placed on the straight line shown in Figure 5. This indicates that the travel times could be attributed to a constant velocity with depth in the mantle out to events with a chord-segment distance of 32.1 degrees.

For a constant velocity with depth the chord segment distances will be the actual travel paths and calculations show 8.1 km/sec to be the velocity which would produce the observed P wave travel times.

Previously the close correspondence between the observed and expected P travel times for events in the 18 to 20-degree range was mentioned. It should be noted that these values also correspond closely to the 8.1 km/sec line. This suggests that the average velocity is around

8.1 km/second. Since the Jeffreys-Bullen model predicts a linear velocity increase with depth starting at 33 km with a velocity of 7.7 km/sec, a velocity greater than 8.1 km/sec must have been encountered for the observed values in the 18 to 20-degree range to average 8.1 km/sec.

As the events become more distant and the travel paths deeper in the earth, the correspondence between the observed and expected travel times no longer holds. The observed values maintain a constant velocity of 8.1 km/sec out to 32.1 degrees.

This region of constant P velocity bounded above by a velocity greater than 8.1 km/sec and bounded below by a rapid velocity increase in the 32.1 degree to 35.1 degree chord-segment distance range establishes a low velocity channel for primary seismic waves.

A similar analysis may be made with the S travel times although their arrivals were not as distinct as the P arrivals, and S waves were not recorded for events beyond a chord segment distance of 32.1 degrees.

For a constant velocity with depth the chord segment distance will be the actual travel path and calculations show 4.65 km/sec to be the velocity which would produce the observed S wave travel times.

In view of the possible 10-second error, it is reasonable to say that the observed and expected S wave travel times may correspond out to a distance of 24.0 degrees. Since these values also are close to the 4.65 km/sec line, an average velocity of 4.65 km/sec is suggested for the expected values. Since the Jeffreys-Bullen model predicts a linear velocity increase with depth starting at 33 km with a velocity of 4.3 km/sec, a velocity greater than 4.65 km/sec must have been encountered

Table 4. Data for P and S Travel Time Curves

Event No.	Chord Segment Distance (degrees)	Observed P Travel Time (secs.)	Expected P Travel Time (secs.)	Observed S Travel Time (secs.)	Expected S Travel Time (secs.)
1	18.0	247.5	251.5	437.5	450.5
2	18.8	257	260	447	466.5
3	19.3	261	262	450	472
4	20.25	279	269.5	491	500
5	20.4	274	274	487	500.5
6	21.6	291	291	NC	--
7	21.5	297.5	285.5	528	515
8	21.85	303	283	NC	--
9	22.3	304	298	537	537.5
10	23.8	323	312	569	560.5
11	24.0	327	314	571	567
12	24.1	329.5	311.5	NC	--
13	27.1	374	346.5	646	642
14	27.15	375	346	653	623.5
15	27.5	380.5	350	657.5	630
16	27.55	378	348	NC	--
17	27.8	382	352	662	634
18	27.85	386.5	352.5	671.5	634.5
19	28.1	383	355.5	670	640
20	28.3	392	354.5	NC	--
21	28.4	382	349	673	629
22	29.1	398	364.5	701	656.5
23	32.05	443.5	389.5	770.5	701
24	35.1	382.5	385	NP	--
25	46.3	515.5	516.5	NP	--
26	49.8	555.5	551	NP	--
27	56.8	565	567.5	NP	--

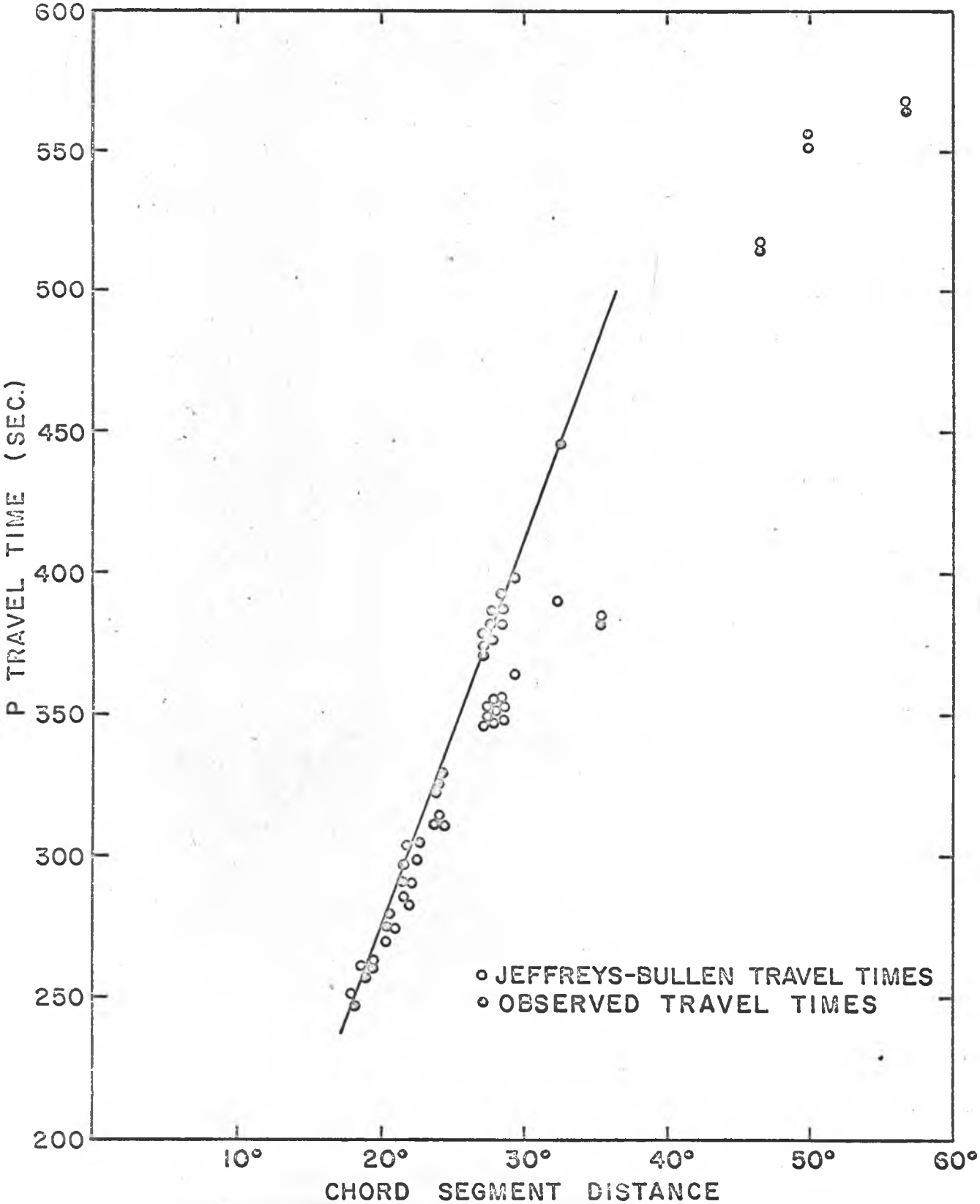

Fig. 5. P Travel Times vs Chord Segment Distances

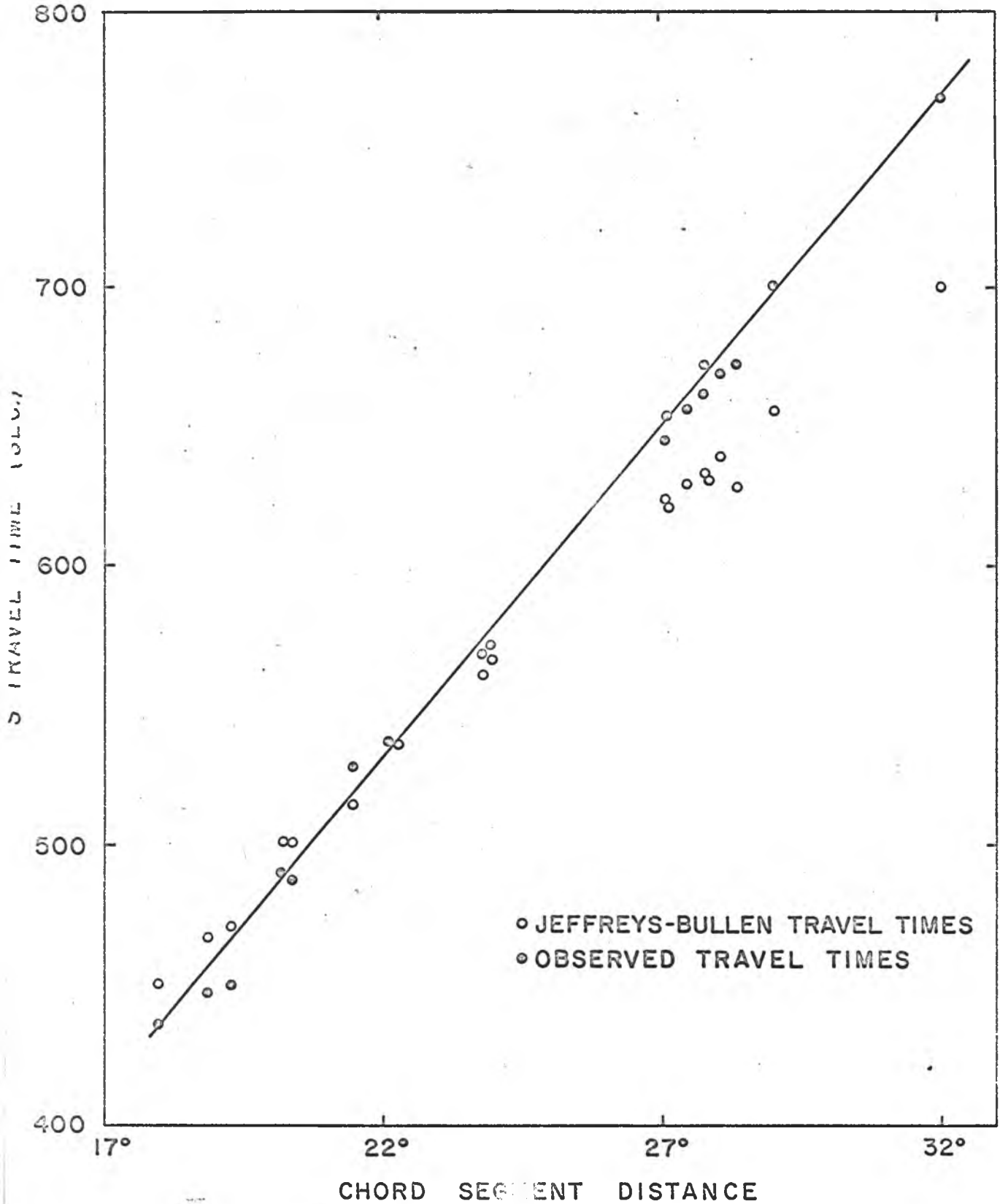

Fig. 6. S Travel Times vs. Chord Segment Distances

for the observed values in the 18 to 24-degree range to average 4.65 km/second.

Although no S arrivals are recorded beyond 32.1 degrees, it is reasonable to assume that somewhere beyond 32.1 degrees the S velocity should be greater than 4.65 km/second.

The region of constant S velocity bounded above by a velocity greater than 4.65 km/sec and bounded below by an unobservable velocity increase beyond 32.1 degrees establishes a low velocity channel for secondary seismic waves.

The Boundaries of the Channel

Of those events which may be useful in determining the upper boundary, events 4 and 5 have particularly distinct first arrivals. Figure 7 is a plot of these events at the appropriate apparent distances from the recording station.

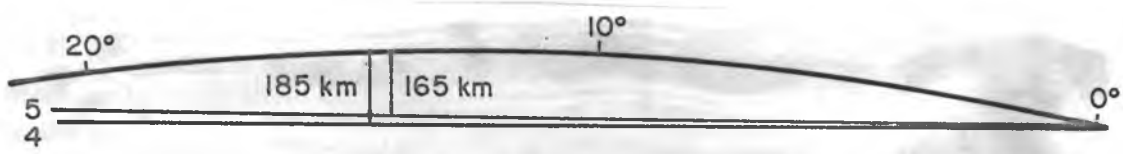

Fig. 7. Events Determining the Upper Boundary

Assuming a linear path, event 5 reaches a maximum depth of 165 km in its travel to the station. Event 4 reaches a maximum depth of 185 kilometers. As it appears from the P travel time residuals that event 5 did not enter the channel whereas event 4 did, it can be condluded that the upper boundary of the P velocity channel lies between 165 km and 185 kilometers.

By a similar analysis it was found that events 3 and 6 had maximum depths of penetration to 155 and 130 km respectively while the residuals indicated that they did not enter the channel. Event 7 reached a maximum depth of 170 km while its residual indicated entry into the channel. These facts support the conclusion that the upper boundary lies between 165 and 185 kilometers.

The events which mark the lower boundary are 23 and 24. The travel time residuals indicate that event 23 had obviously travelled in the channel while 24 occurred below the channel. Since for a linear path the maximum depth of penetration of event 23 is 290 kilometers and the focal depth of 24 is 542 kilometers, it is concluded that the P velocity channel ends at a depth greater than 290 kilometers but less than 542 kilometers.

Since no S phases were found to be comparable to the P phases of events 4 and 5, no attempt was made to find the S channel's upper bound. Since no S arrivals were observed beyond a chord segment distance of 32.1 degrees, the S channel's lower bound could not be established. It is not unreasonable to suppose that the S channel boundaries may be similar to the P channel boundaries.

The Herglotz-Wiechert Method

The Herglotz-Wiechert method of depth determination was not used to estimate the boundaries of the low-velocity channel; it has been shown to be applicable to velocity decreases with depth provided the following condition is satisfied:

$$\frac{dv}{dr} < \frac{v}{r}$$

where "v" is the velocity at any depth, "r" is the distance from the center of the earth to that depth, and "$\frac{dv}{dr}$" is the rate of change of velocity with depth at that depth. The Herglotz-Wiechert method was not used because a fundamental condition was not satisfied. A condition for the applicability of the Herglotz-Wiechert method is that the apparent surface velocity is a monotonically increasing, continuous function of distance (Macelwane, 1949, p. 181). In order to determine whether this condition was satisfied under the present study, all events were projected to a more distant zero focus event by assuming a linear (chord-segment) travel path. As shown in Figure 8, the assumed travel path was projected from the focus "C" to its intersection with the surface of the earth "A". To determine the travel time spent on the additional travel path segment "B", a P-wave velocity of 8.0 km/sec was assumed, the linear distance of the additional path segment was measured and the additional path segment was obtained by dividing this distance by the assumed 8.0 km/sec velocity.

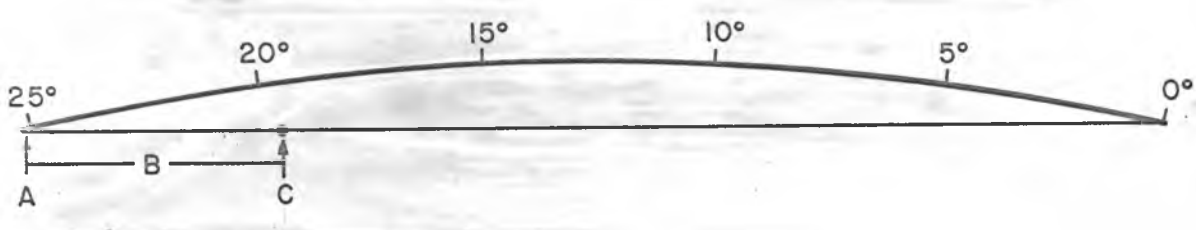

Fig. 8. Reducing Events to Zero Focus

The apparent surface velocity was obtained by dividing the new zero focus apparent distance by the sum of the additional and observed travel

Table 5. Data for Events Projected to a Zero Focus

Event No.	New Apparent Distance (degrees)	Additional Distance (degrees)	Additional Time (secs.)	Observed Time (secs.)	New Travel Time (secs.)	Apparent Velocity (km/sec)
1	19.7	1.6	22.2	247.5	269.7	8.12
2	21.95	2.95	41.0	257	298	8.19
6	23.4	1.6	22.2	291	313.2	8.30
9	24.2	1.75	24.3	305	329.3	8.17
3	25.2	5.6	77.8	261	338.8	8.27
5	25.9	7.2	73.7	274	347.7	8.28
10	26.3	2.2	30.6	323	353.6	8.27
7	26.6	4.8	66.7	299	365.7	8.09
11	27.05	2.7	37.5	329.5	367.0	8.20
4	27.8	7.2	100.1	279	379.1	8.15
12	28.45	3.8	52.8	331.5	384.3	8.23
13	28.85	1.2	16.7	374	390.7	8.21
15	29.0	1.1	15.3	380.5	395.8	8.15
14	29.4	1.8	25.0	374.5	399.5	8.18
17	29.7	1.45	20.2	382	402.2	8.21
19	29.9	1.35	18.8	382	400.8	8.30
18	30.25	1.8	25.0	383.5	408.5	8.23
16	30.3	2.2	30.6	378	408.6	8.25
8	30.5	8.2	114.0	303	417.0	8.13
20	30.9	2.2	30.6	391.5	422.1	8.14
22	31.0	1.4	19.5	398	417.5	8.26
21	33.75	4.8	66.7	382	448.7	8.36
23	34.4	1.8	25.0	443.5	468.5	8.16

times. A summary of these calculations is given in Table 5. A comparison of the apparent distances to the apparent velocities shows that the condition of monotonically increasing apparent velocity is not satisfied. Hence, the Herglotz-Wiechert method was not applicable.

Dowling and Nuttli (1964) suggest a method by which travel times for an assumed earth model can be computed. Since a model for the Northwestern Pacific could only be estimated at this time, the method of Dowling and Nuttli was not used. Under NSF contract GP-3437, the Hawaii Institute of Geophysics has undertaken to obtain a more detailed crustal and upper mantle model. It is hoped that in that study a method such as Dowling and Nuttli's may be used to correlate body and surface wave models.

Summary and Conclusions

The purpose of this investigation was to study the velocity of the upper mantle below the Northwestern Pacific, and, if a low velocity channel existed, to obtain some knowledge of its boundaries.

The norms used to indicate its existence were travel time residuals and Jeffreys-Bullen travel times. Since the observed travel times were significantly greater than the expected Jeffreys-Bullen values in the 21 to 33-degree range, the existence of a low velocity channel was suggested. The channel was established for both P and S waves by an analysis of the observed and expected travel times.

For primary seismic waves the upper bound of the channel seems to be between 165 km and 185 km, and the velocity in the channel constant at 8.1 km/second.

For secondary seismic waves the velocity in the channel appears to

be constant at 4.65 km/second. The boundaries for the secondary waves were indeterminate.

Acknowledgments

The author thanks the Pacific Missile Range System for providing the hydrophone records; Rockne Johnson and Roger Norris of the Hawaii Institute of Geophysics T-phase study group for bringing the body wave arrivals to his attention; G. Lafayette Maynard for his comments and encouragement; and Dr. George P. Woollard for carefully reviewing this report. The author thanks Mrs. Ethel McAfee for her editorial help. This research was supported in part by the National Science Foundation under contract GP-3437.

References

Anderson, Don L., and M. Nafi Toksoz, 1963, "Surface Waves on a Spherical Earth," J. Geophys. Research, 68, pp. 3483-3499.

Dorman, James, Maurice Ewing, and Jack Oliver, 1960, "Study of Shear Velocity Distribution in the Upper Mantle by Mantle Rayleigh Waves," Bull. Seismol. Soc. Amer., 50, pp. 87-115.

Dowling, John, and Otto Nuttli, 1964, "Travel-Time Curves for a Low-Velocity Channel in the Upper Mantle," Bull. Seismol. Soc. Amer., 54, pp. 1981-1996.

Ewing, Maurice, James Brune, and John Kuo, 1962, "Structural Features of the Pacific," Crust of the Pacific Basin, AGU, Geophysical Monograph No. 6, pp. 30-40.

Jeffreys, Harold, and K. E. Bullen, 1958, Seismological Tables, Office of the British Association, Burlington House, W. 1, London.

Kovach, Robert L., and Don L. Anderson, 1964, "Higher Mode Surface Waves and their Bearing on the Structure of the Earth's Mantle," Bull. Seismol. Soc. Am., pp. 161-182.

Macelwane, James B., 1949, Introduction to Theoretical Seismology, Part I, Geodynamics, St. Louis University Press, St. Louis, Missouri.